MECHANICAL AND ELECTRICAL PROPERTIES OF 3D PRINTED PA6 NANOCOMPOSITES

Jitendra S. Tate[1,2], Oluwasola K. Arigbabowo[2], Micheal LePere[2],
Henry Okeke[2], Jesse Garcia[2], and Aziza Nahar[2]

Texas State University
San Marcos, TX, 78666
[1]Materials Science, Engineering and Commercialization Program, Texas State University
[2]Ingram School of Engineering, Texas State University
Phone: 512-245-4872; Fax: 512-245-7771
Email: JT31@txstate.edu

ABSTRACT

Polyamide 6 (PA 6) nanocomposites are viable engineered nanocomposite materials with potential application in electrostatic discharge dissipation applications. Creating an electrically conductive path to dissipate electrostatic charges in such materials can be a viable solution to Electrostatic Discharge (ESD) concerns. The addition of nanofillers can also enhance mechanical properties of the parent polyamide 6, a structural thermoplastic ideal for 3D printing via fused deposition modelling (FDM). While improving the ESD capability, it is imperative to sustain the structural integrity of the nanocomposites. Hence, this study evaluated the mechanical, thermal and electrical properties of 3D printed PA6 Nanocomposites for electrostatic discharge applications. 3 and 5 wt.% of Carbon Nanofiber (CNF) was compounded with PA6 using co-rotating twin screw extruder) to produce 1.75mm diameter monofilaments for fused deposition modelling (FDM). The test samples were printed using commercial-off-the-shelf (COTS) 3D printer, Lulzbot TAZ 6 FDM printer. Mechanical, electrical and thermal characterization were carried out according to their respective ASTM standard. The tensile and flexural properties were enhanced by 3wt% addition of CNF, but no significant improvement was observed at 5wt%. The CNF nanocomposites exhibited good thermal stability and crystallization phenomenon at both loading levels. The volume resistivity of the PA6 matrix was reduced to order of 10^{11} and 10^{12} by 3wt% and 5wt% CNF addition respectively, which seems promising for manufacturing static discharge products.

Key Words: Polyamide 6, Carbon Nanofiber-CNF, Nanocomposites, Fused Deposition Modelling- FDM, Additive manufacturing

1. INTRODUCTION

Polyamides (PA) are known engineering thermoplastics with remarkable combination of mechanical, thermal and manufacturability properties for diverse applications. Depending on the composition of their main chain, polyamides have been widely categorized as either aromatic or aliphatic polyamides [1]. Aromatic polyamides, also referred to aramids, are high performance materials that possess beneficial properties such as low moisture sensitivity, oxidation resistant, excellent thermal and mechanical properties. However, they are very expensive, and their applications are limited to very demanding applications e.g. Nomex® and Kevlar® utilized in bullet proof vest and military body armor[2]. Aliphatic polyamides are the widely used polyamides for engineering and industrial applications. They belong to a family with the generic name of "Nylons" and are manufactured via condensation of copolymers obtained from the reaction between equal molecules of diamines and dicarboxylic acid. Nylon are semi crystalline in nature with presence of both crystalline and amorphous phases. They possess exceptional mechanical, wear and crystallinity properties that is widely exploited in a wide range of applications in commercial fibers, transportation, sports, electronics and automotive industries[3]. The common types of Nylons (aliphatic polyamides) are PA 12, PA11, PA 6,6 and PA 6.

Polyamide 6 (PA 6) is one of the most widely utilized thermoplastics in manufacturing. It is a cost effective and suitable material choice in producing end use functional parts via Additive Manufacturing, also known as 3D printing- creating parts layer by layer from a 3D geometrical model. It affords advantages of overall cost efficiency, flexibility and manufacturability of custom polymers without jeopardizing their intrinsic properties. Aside from being an ideal 3D printing material, easy modification of PA 6 has made them practical for vast uses and promising applications[4]. Despite their great potential in offering excellent thermal and mechanical properties, the lack of mobile electron carriers, typical of polymeric materials, has been a major drawback in expanding its use in applications demanding for good electrical properties. This can be addressed by creating a three-dimensional low resistance network for electron flow and modifying the Polyamide 6 matrix with conductive nanoparticles could be considered a plausible solution for electromagnetic shielding (EMI) and electrostatic discharge (ESD) concerns. Carbon fillers such as carbon black, carbon nanotubes (CNT), nanographene platelets (NGP) and carbon nanofiber (CNF) have been identified to be viable in this regard and incorporations of these fillers into PA 6 matrix could results in a novel type Polyamide 6 nanocomposites.

Bauhofer (2009) reported that the PA6 percolation threshold could be achieved at loading levels as low as 2.5wt.% or higher CNT loading [5]. Percolation threshold, as illustrated in Figure 1, is the minimum quantity of filler required to form a conductive path within the polymer. Furthermore, Zonder *et al.* (2011) affirmed that PA 12 can better disperse CNT due to its polar nature and electrical and rheological percolation was achieved around 1.4wt% CNT. This ability has been attributed to the large aspect ratio (length-diameter) typical of fillers such as carbon nanotubes and carbon nanofibers fillers[6]. In the work of Gaikwad *et al*. (2013), where NGP was

successfully dispersed in PA11 using co-rotating twin-screw extruder, the percolation threshold was achieved at 7wt% NGP. They emphasized that manufacturing method of composites plays important role in percolation threshold as it affects orientation, dispersion, aspect ratio of filler and interparticle spacing within the polymer matrix [7].

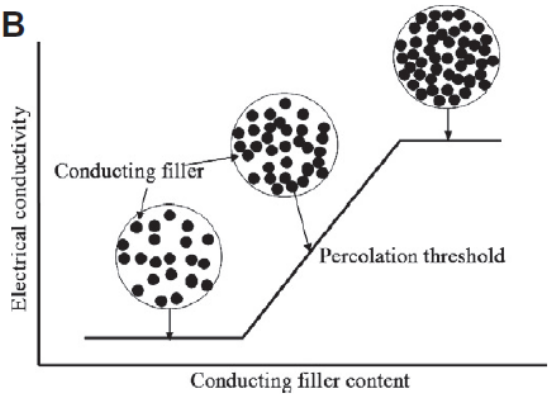

Figure 1: Percolation Phenomenom in Conducting Composites [8]

Carbon nanofibers has been identified to enhance the stiffening of thermoplastics matrix. It has the ability to improve the thermal and thermo-oxidative stabilities of the polymer matrix, and dispersion of CNF was reported to have acted as nucleation sites, thereby leading to formation of new crystalline domains [9, 10]. According to Goodridge (2011), the improvement in tensile properties obtained via laser sintering of PA12/Carbon Nanofiber (CNF) composites was attributed to the high aspect ratio of the nanofibers. Aspect ratio is the proportional ratio of length to diameter of the fibers. The diameter of CNF ranges between 20- 200nm which are quite larger than that of carbon nanotubes (2-100 nm) and their length can be more than a micron, resulting into high aspect ratio of CNF and CNT > 100 [11-13]. In addition to the low density and high aspect ratio of CNF, it has been considered more economical than CNT in terms of manufacturability and monetary cost [13], thereby proving more viable in developing advance nanocomposites. Hence, this paper was aimed to develop a carbon nanofiber polyamide 6 composite which could be viable for 3D printing and to evaluate the mechanical, thermal and electrical performance of CNF/PA6 nanocomposites.

2. MATERIALS SYSTEM AND MANUFACTURING

2.1 Materials System

Nylon 645, a thermoplastic monofilament that is ideal for fused deposition modelling 3D printing was chosen as the polymer matrix for the nanocomposites. Nylon 645 is a copolymer that consists of the purest form of a delta transition of Nylon 6/9, Nylon 6 and Nylon 6T, which is manufactured

by Taulman 3D. Also, it possesses a high chemical resistance and is highly compatible in application where Nylon 6 and Nylon 6,6 are required**.**

The nanoparticles used for polymerization in this study were pyrograph III, PR-24-XT-LHT grade. The LHT grade is a low heat treated (LHT) carbon nanofiber grade which has been carbonized chemically by heating to temperatures of 1500°C to deposit the carbon present on the surface of Pyrograf®[14]. This heat treatment produces nanofibers which generally provides the highest electrical conductivity in nanocomposites. Pyrograph III-carbon nanofibers has a nanofiber density of 1.55 to 1.70 g/cc. Carbon nanofibers possess high length to diameter ratios which is essential for achieving an electrical resistivity near the percolation threshold and can be viable to develop nanocomposites for static dissipation applications. In addition, its lower cost per pound as compared to other conductive nanofillers such as carbon nanotubes makes it more economically viable. Carbon nanofibers are also considered for the enhancement of the mechanical properties of the polymer matrix as carbon nanofibers also contain excellent intrinsic mechanical properties.

2.2. Melt Compounding

The polymer nanocomposite was compounded via twin screw extruder. This was achieved with the help of Process 11 twin-screw extruder manufactured by Thermo Fisher Scientific. The compact co-rotating 11mm twin screw extruder is designed with a unique monocoque housing that is suitable for compounding thermoplastic polymers. In addition to its water-cooled primary feed port it contains 3 multifunction barrel ports for additional feeding and venting. Its barrel is separated into 8 sections to facilitate temperature profiles. The L/D ratio of this extruder is 40.

The extruder possesses an intermeshed co-rotating twin screws capable of both distributive and dispersive mixing into a homogeneous mass in a continuous process. There are 8 heating zones along the extruder barrel and the temperature profile employed from the primary hopper to the die are: 245^{o}C, 250, 250 ^{o}C, 255 ^{o}C, 255 ^{o}C, 255 ^{o}C, 255 ^{o}C, 255 ^{o}C. The twin screws rotation rate was set to an optimized value of 150 rpm. The Nylon 645 was fed through the primary hopper while the Pyrograf III was side fed via the secondary hopper along the extruder barrel. The setup is shown in Figure 2 below.

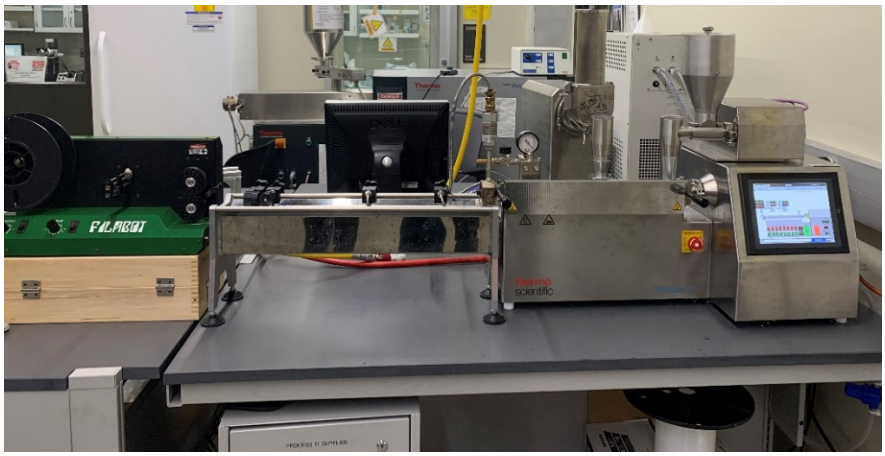

Figure 2. Twin Screw Extruder (11mm diameter)

2.3 Fused Deposition Modelling

The 3D printer used to print nanomodified filament samples was a LulzBot TAZ™. The LulzBot TAZ™ was used to print tension, flexural, dynamic mechanical analyses, and resistivity test samples of carbon nanofiber modified Nylon at weight percentages of 0%, 3%, and 5%. Because Nylon 6 has a melting temperature of 207ºC, a printing temperature between 255 ºC and 260 ºC were selected to ensure proper deposit viscosity for the filament to adhere to the bed and to itself. To ensure the foundation print was successful, we selected the bed temperature of 100 ºC to get the nylon to adhere to the bed properly. To ensure the filament prints around the perimeter of the test specimens well, we have selected an outer edge fill speed to be half of that of the infill speed since less nylon filament adhere to on the edges of the specimen than that of the infill. We have also selected a nozzle with diameters ranging from 0.4mm to 0.8mm due to the high length to width aspect ratios of the carbon nanofibers extruding from the nozzle which can lead to clogging.

3. EXPERIMENTATION

3.1 Mechanical Characterization

Total five tension samples were printed according to ASTM D638-Standard Test Method for Tensile Properties of Plastics [15]. The tensile dog bone specimen “Type 1” has overall length, overall width and thickness as 165mm, 19mm, and 3.2mm, respectively. The tensile testing was performed as shown in Figure 3 using United Testing Machine (UTM) with a 50kN loading capacity (11 kips) and the strain values were collected using 2 inches gauge length extensometer with a measuring accuracy of 0.0002. The force-extension data was generated using the Datum 5i software of the UTM and tensile properties were evaluated.

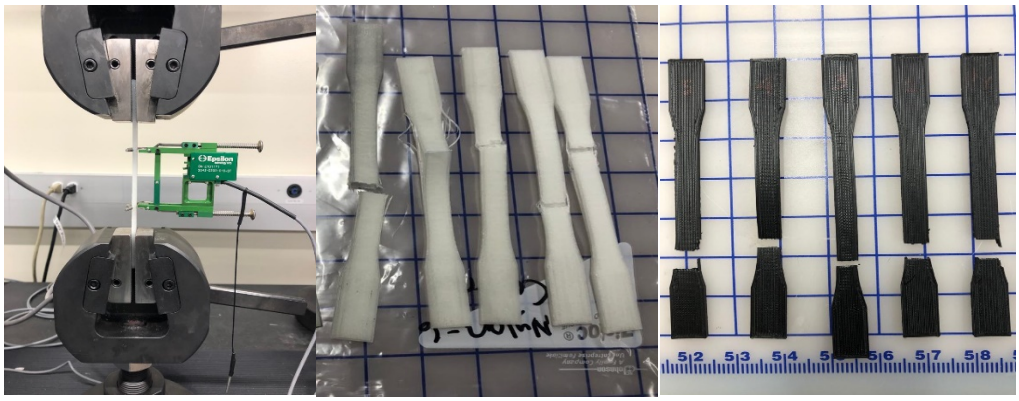

Figure 3: Tension test of 3D printed PA6/CNF nanocomposites

Total five flexural samples were printed and subjected to a 3-point bed test according to "ASTM D790- Standard Test Methods for Flexural Properties of Unreinforced and Reinforced Plastics and Electrical Insulating Materials" [16]. The flexural samples with a dimension of 12.7 mm wide, 3.2 mm thick, and 127 mm long were tested on the support span (span-to-depth ratio) of 16:1.These tests were performed according to Type I, which utilized the cross head position as the deflection measurements and Procedure B was followed, which is designed principally for those materials that do not break or yield in the outer surface of the test specimen within the 5.0 % strain limit when Procedure A conditions are used.

3.2 Electrical Testing

The electrical resistivity of control and nanomodified samples was measured according to ASTM D257 – "Standard Test Methods for DC Resistance or Conductance of Insulating Materials [17]. This is to evaluate the volume resistivity of the CNF conductive fillers. The test samples printed were circular disks with a dimension of 1mm thickness and 88.9 mm diameter. The volume resistivity was determined by Keithely Megohmeter setup comprising the Keithely 2450 source meter, Keithely 6514 Electrometer and the Linear four-point probe (Jandel Universal Probe) for housing the test sample. Voltage varying from 10V to 120 V was applied using the source meter for an electrification time of 60 seconds and the amount of current flowing was sensed by the electrometer. The volume resistivity values were evaluated according to Equation 1 below;

$$\rho_v = k_v * \frac{R}{t} \qquad (1)$$

Where $\rho_v =$ volume resistivity ($\Omega.\,cm$),

$k_v =$ effective area of the circular electrode $= 22.881\ cm^2$,

R = measured resistance (Ω), and t = sample thickness (1mm).

3.3 Thermal Analysis

The material thermal stability was evaluated via ASTM - Standard Test Method for Thermal Stability by Thermogravimetry [18]. This was to determine the decomposition temperature of the materials and the degree of mass change via thermogravimetry. The mass of the sample was about 7.5mg for nanomodified composites. The samples were placed inside an alumina pan at ambient temperature after zeroing an empty and clean specimen pan. The test material was heated from ambient temperature to 600 ^{o}C at a rate of 10 ^{o}C /min. The testing material was heated in an alumina pan and maintained under inert atmosphere of 99.9% purity, purging the inert gas (Nitrogen) at a rate of 50 ml/min.

Thermal transitions of the nanomodified polyamide 6 were investigated via ASTM D3418-15- Standard Test Method for Transition Temperatures and Enthalpies of Fusion and Crystallization of Polymers by Differential Scanning Calorimetry (DSC)[19]. This test method was employed to evaluate the glass transition temperature, peak crystallization temperature and melting point of the material. The testing procedure was a single testing as discussed in the thermogravimetry procedure and was carried out with the aid of simultaneous differential thermogravimetry (SDT) analyzer capable of both TGA and DSC. The DSC sensing device of the SDT was used to monitor the difference in heat input between a reference material and a test material due to energy changes in the material, thereby resulting into different exothermic valleys and endothermic peaks, indicating different thermal transitions.

Dynamic mechanical data of the carbon nanofiber modified polyamide 6 was investigated according to ASTM D4065- Standard Practice for Plastics: Dynamic Mechanical Properties: Determination and Report of Procedures [20]. This test was aimed to determine the viscoelastic characteristics of the material by monitoring the elastic and loss modulus as a function of temperature. A rectangular cube with dimension 35mm X 12mm X 3 mm, maintained at a temperature of 23^{o} C was subjected to a mechanical oscillation of a frequency of 1 HZ in a single cantilever test mode. The material was taken through a temperature ramp from 23^{o} C to 200^{o} C at a rate of 5 ^{o} C/min via a Dynamic Mechanical Analyzer equipment TA- DMA 2980 and the obtained data was analyzed using Universal Analysis Software.

4. RESULTS AND DISCUSSION

4.1 Mechanical Properties

The mechanical response of the investigated material is of prime importance in quantitatively evaluating the structural integrity of the developed 3D printing nanocomposite filaments. This could prove viable as a fabricating 3D printing filament for end use industrial products, thereby replacing injection molded parts. The mechanical properties evaluated are the tensile and flexure properties as presented in Table 1

Table 1: Mechanical Properties Data

	0 wt.% CNF	3 wt.% CNF	5 wt.% CNF
Ultimate Tensile Strength (MPa)	37.21 (2.108)	41.44 (1.836)	30.14 (6.512)
Tensile Modulus (GPa)	1.574 (0.074)	2.943 (0.905)	1.559 (0.171)
Percentage of Elongation (%)	78.90 (0.055)	46.30 (0.107)	34.45 (0.229)
Equilibrium Toughness (MJ/m^3)	1.46 (0.158)	2.05 (0.649)	1.20 (0.083)
Flexural Strength (MPa)	33.93 (5.331)	39.54 (3.340)	40.39 (6.530)
Flexural Modulus (GPa)	0.768 (0.133)	1.130 (0.115)	1.173 (0.243)

***Standard Deviation in Parenthesis**

The trend in the observed tensile and flexural strength are presented graphically in Figure 4 below. In Figure 4a, tensile strength was observed to have appreciably increase at 3wt% CNF inclusion, which decreases as the CNF concentration was increased to 5wt%. It is well understood that high aspect ratio fillers like CNF and CNT prove difficult to disperse homogeneously because of their high surface area and a strong inclination to agglomerate [21]. Due to this reason, high shear dispersion techniques like twin screw extrusion has been recommended. However, the high shearing action associated with this technique could truncate the long fibers, thereby reducing its aspect ratio below a critical value. This could explain the deterioration of tensile strength observed at 5wt%. Although the tensile strength depreciates at 5wt%, the continuous improvement in the flexural strength of the nanocomposites, as shown in Figure 4b, is an indication that inclusion of CNF could prove viable in enhancing mechanical properties. These mechanical strengths indicators are closely related as they both measures the resistance to deformation depending on the type of applied load.

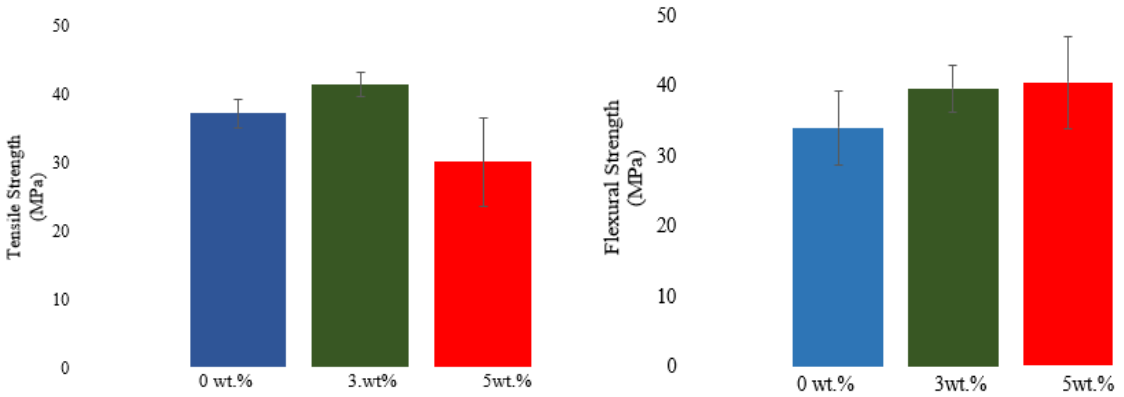

(a) *(b)*

Figure 4: Tensile and Flexural Strength of 3D printed PA6/CNF nanocomposites

Barrick (2011) reported that improvement in tensile properties of nanocomposites is dependent on the aspect ratio and the nanofiber-matrix interfacial strength. As shown in Figure 5a, the addition of 3wt.% CNF exhibits a strong reinforcing and stiffening effect of the Nylon and the enhancement observed in tensile modulus could be attributed to a strong interfacial strength which effects an efficient load transfer from the matrix to the reinforcement [22]. By increasing to 5wt% CNF inclusion, no appreciable effect was observed in tensile modulus, however the nylon matrix was increasingly stiffened by increasing CNF contents under bending load as shown in the flexural modulus plot in Figure 5b. The spatial orientation of CNF significantly impedes the movement of the amorphous phase of the Nylon matrix, thereby resulting into the stiffening of the material. It is noteworthy that higher loading levels is prone to entanglements of the fibers, promote agglomeration and consequently deteriorates the stiffness of the nanocomposites. Therefore, it is imperative to optimize the processing parameters of the extrusion process to maximize the reinforcing ability of CNF at high loading levels, like 5wt.% and above.

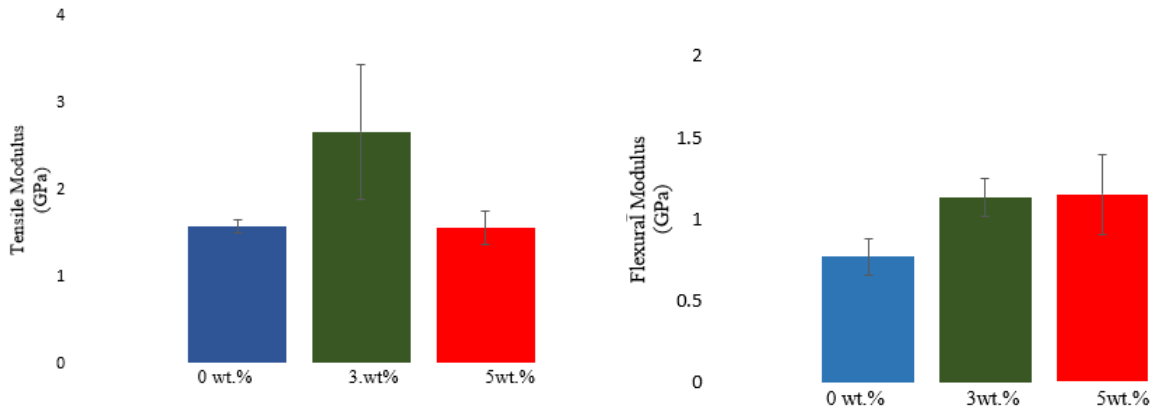

(a) *(b)*

Figure 5: Tensile and Flexural Modulus of 3D printed PA6/CNF nanocomposites

Figure 6 presents the trend in percentage (%) elongation and toughness of the investigated material. The percentage elongation reduces drastically with increasing CNF loading as presented in Figure 6a. % elongation is an indication of the ductility of the material and the continuous decline could be attributed to the restriction in the polymer chain movement. This restriction has been suggested to be due to the reduction in the free volume capacity of the Nylon 6 [22].

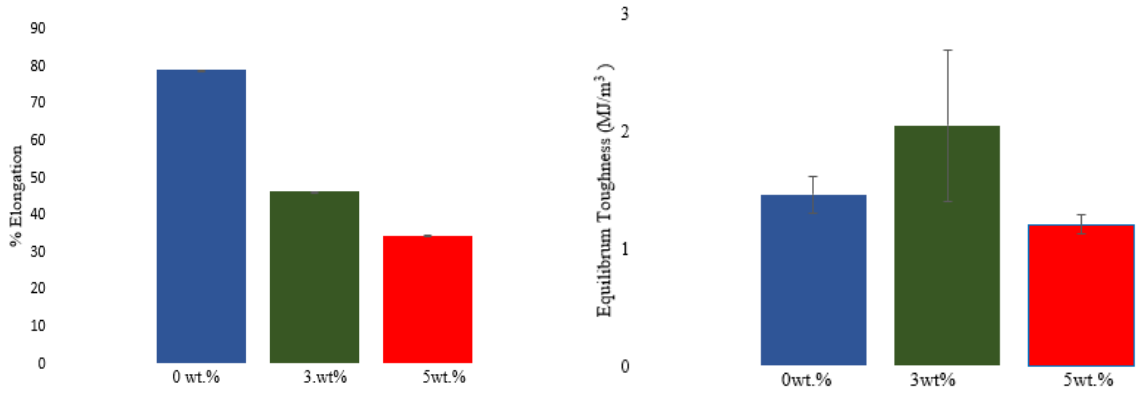

(a) *(b)*

Figure 6: % Elongation and Toughness of 3D printed PA6/CNF nanocomposites

Figure 7 shows the tensile stress versus tensile strain plots which was obtained by integrating from zero to elongation at break to illustrates the area under the tensile curve. The area under the stress-strain curve was evaluated as the equilibrium toughness as shown in Figure 6b, which represents the total strain energy per unit volume that was induced by the applied stress. The similarity in the trend showed in the equilibrium toughness and tensile strength is an indication of the close relationship between the two tensile properties, which explains the fact that maximizing the strength is parallel to improving the toughness of the nanocomposites.

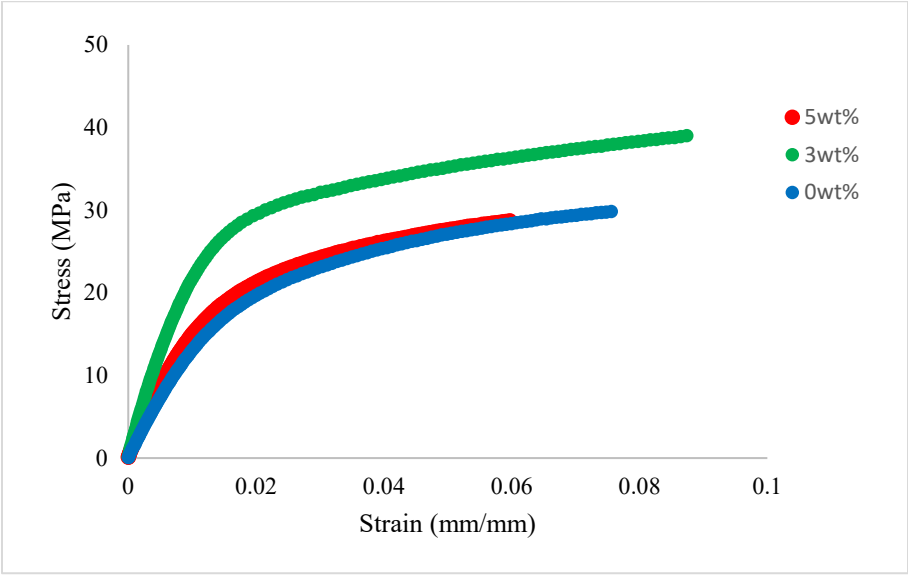

Figure 7: Tensile stress vs Axial strain of 3D printed PA6/CNF nanocomposites

4.3 Volume Resistivity

Table 2 presents the volume resistivity data collected in an electrical resistivity testing by varying the voltage source from 10 -120 v. The primary importance of the volume resistivity measurement was to evaluate how the carbon nanofiber impart the conductivity of the Nylon matrix which could prove viable in low resistivity applications such as static dissipation. The reduction in the resistivity of the nylon matrix was achieved via the attainment of a percolation nexus of CNF, which creates a conductive pathway throughout the matrix, thereby facilitating electron transfer [23].

Table 2: Volume Resistivity Values

	Resistivity (Ohm.cm)		
Voltage (V)	**3wt%**	**5wt%**	**0wt%**
10	6.21E+11	1.75E+12	5.40E+13
20	6.27E+11	1.52E+12	5.40E+13
30	7.79E+11	1.43E+12	5.40E+13
40	7.04E+11	1.38E+12	5.40E+13
50	7.33E+11	1.36E+12	4.35E+13
60	7.30E+11	1.33E+12	4.46E+13
70	5.46E+11	1.32E+12	4.48E+13
80	5.16E+11	1.30E+12	4.55E+13
90	5.08E+11	1.29E+12	4.40E+13
100	5.23E+11	1.31E+12	4.45E+13
120	5.06E+11	1.30E+12	4.30E+13

It could be observed in Figure 8 that the volume resistivity of the Nylon 6 matrix in the order of 10^{13} was lowered to the order of 10^{11} and 10^{12} for 3 and 5 wt.% respectively. In CNF nanocomposites, the tunneling effect facilitated by the high aspect ratio of the filler has been identified as the main mechanism of electrical conduction[24]. The observable reduction in the resistivity could be as a result of a conductive network being formed by the CNF, where electrons can tunnel along the length of one filler to another, thereby overcoming the high resistance imposed by the nylon matrix. In order to maximize the conductive ability of CNF, it is imperative to maintain its high aspect ratio. This could give an insight into the slight decrease of resistivity value observed at 3 wt. and 5wt.%. It is suspected that the CNF could have suffered from high shear forces of the twin-screw compounding process, resulting into shortening of the long fibers and consequently delaying the onset of electrical percolation. Although, the results obtained does not reflect a significant influence of the conductive CNF, the resistivity of 3wt.% still falls within the allowable resistivity values for ESD compliance rated between 10^{10} -10^{12} ohms.cm [25].

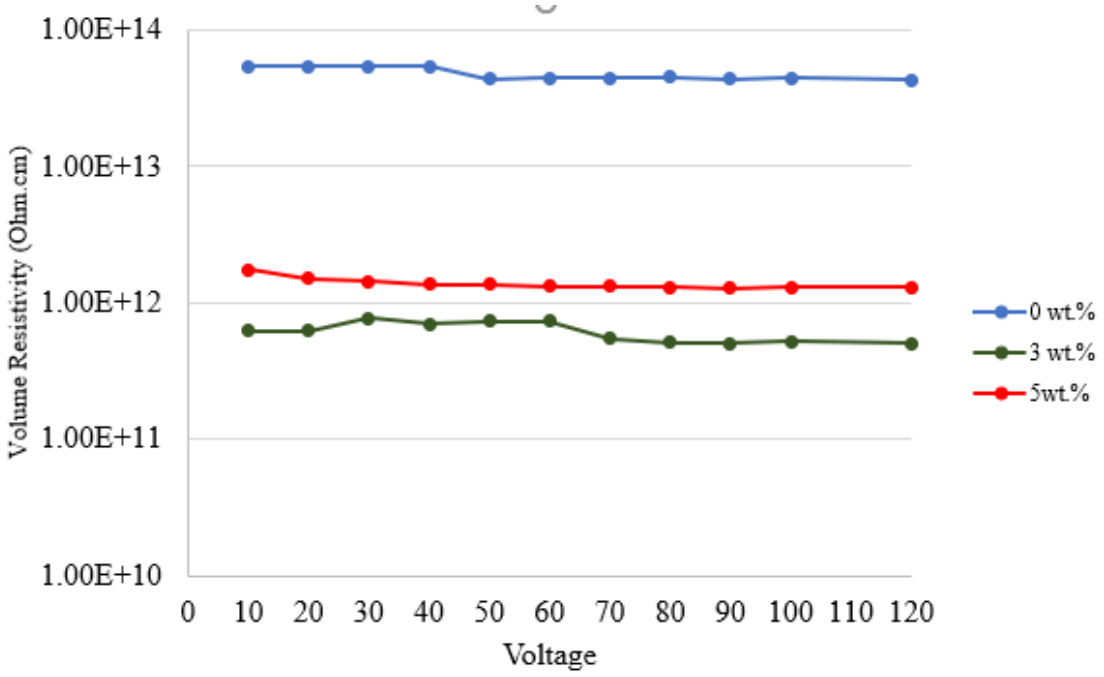

Figure 8: Volume resistivity of 3D printed PA6/CNF nanocomposite

4.4 Thermogravimetric Analysis

The thermogravimetric analyses (TGA) illustrates the thermal stability by measuring the weight loss as a function of temperature. TGA is of prime importance in evaluating the thermal stability of the nanocomposites. There is a close relationship between the thermal stability and the structural integrity of materials which require understanding the decomposition kinetics of our material in a temperature-controlled environment.

Table 3: TGA data

Thermal properties	0 wt.% CNF	3 wt.% CNF	5 wt.% CNF
Decomposition Temperature	400.95	402.53	402.68
Weight % loss	97.738%	97.357%	96.832%

The TGA curve in Figure 9 shows the onset decomposition temperature and the weight percent loss at the end of the heating profile. The extrapolated onset temperature signifies the temperature at which the weight loss begins which is an indication of the thermal stability of the material. The observed slight increase in thermal stability with increasing CNF content could be attributed to the restriction of the Nylon macromolecules by the network structure of the CNF. The intrinsic high thermal conductivity of CNF prevented any sort of heat accumulation and conducts heat uniformly, thereby increasing the thermal stability of the Nylon matrix. In addition, strong interfacial adhesion has been identified as a reason for the thermal stability of CNF based nanocomposites[21]. Strong interfacial bonds prevent the occurrence of interstices that could occur under thermal stresses

where the diffusion of volatile gases from the decomposing material is prominent. However, the interface is prone to interstices buildup at higher CNF loading. Furthermore, no major degradation was observed with inclusion of CNF on the TGA curve and the thermal stability of the nanocomposites was sustained throughout the scanning temperature. The weight loss percentages at the final temperature reduces with increasing CNF loading and the pristine nylon being the highest with 97.738%. The reduction in weight loss observed in the nanocomposites could be ascribed to the restriction imposed by the CNF network structure, preventing the mobilization of the gaseous nylon macromolecules to encounter outer atmosphere during degradation [26].

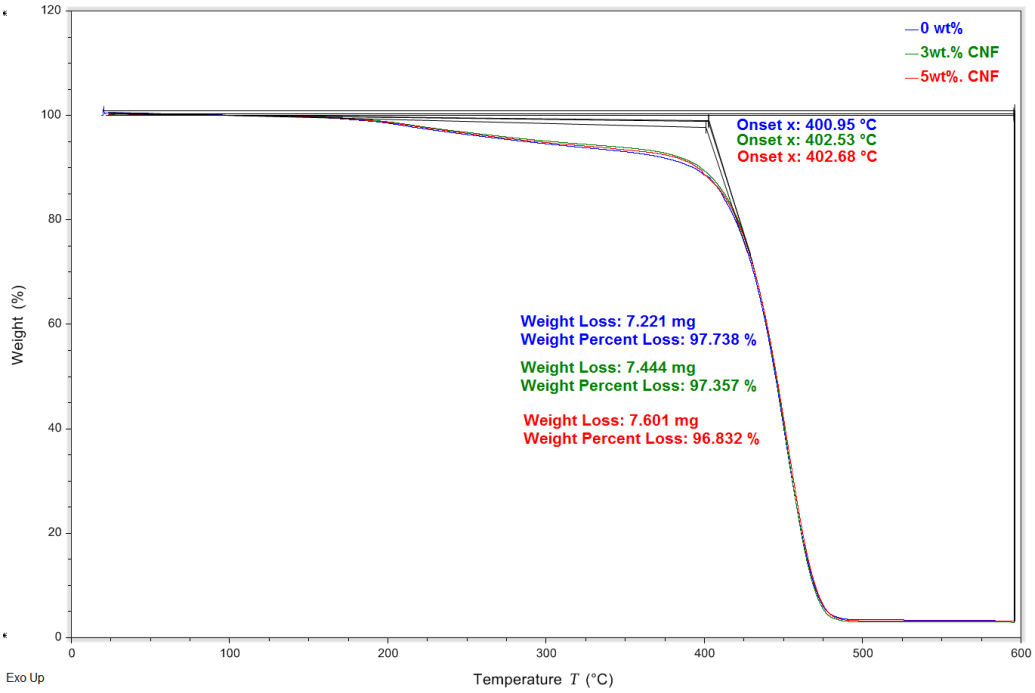

Figure 9: TGA curve of PA6/CNF nanocomposites

4.5 Differential Calorimetry

Table 4 highlights the thermal transition obtained in the differential calorimetry (DSC) first heat cycle of the investigated material. DSC is an important technique that can be used to qualitatively and quantitatively characterize the thermal transitions unique to a material.

Table 4: DSC Thermal transition

Transition parameters	0 wt.% CNF	3 wt.% CNF	5 wt.% CNF
Glass Transition temperature	59.39	60.35	59.93
Peak crystallization temperature	171.61	167.42	166.81
Melting temperature	214.35	213.31	213.32
Heat of crystallization	52.53	77.34	77.43
Degree of Crystallinity	22.8	34.6	35.4

Figure 10 presents the DSC scan obtained in the calorimetry study. The first observable signal on the DSC scan is the glasssy region which signifies the temperature region where the armouphous portion of the material is moving from a glassy to a rubbery state. The glass transition temperature (T_g) of the neat matrix occurs at 59.93^{o}C and a minimal increase to 60.35 and 59.93 ^{o}C was observed at 3 and 5 wt.% reinforcement respectively. Dispersion of CNF within the Nylon matrix led to reduction in free volume movement of the polymer macromolecules due to the restriction imposed by the CNF, thereby delaying the onset of glass transition. The slight increase in T_g of the amorphous region of the Nylon/CNF composites is an indication of the polymer molecules interlocked into a rigid amorphous structure which could possibly translate to the enhancement of the mechanical properties of semicrystalline nylon matrix. In a semicrystalline polymer like Nylon, the armouphous region is reported to be responsible for the elasticity phenomenom [27]. During applied tensile stress, the amorphous molecular chain deforms elastically and the crystalline domains remains undisturbed until yielding begins. The presence of this armouphous region delays the onset of the plastic deformation of the crystalline phase, thereby resulting in the improvement of the strength and modulus of the semicrystalline polymer. Furthermore, the T_g could be used to predict the service temperature of polymeric materials depending on application and desired physical properties, especially for fully armouphous polymers. However, it is noteworthy that the Nylon 6, a semicrystalline polymer, being investigated in this study does not softening even above the T_g . This could be attributed to the presence of relatively strong intermolecular forces which is more sensitive to higher temperature, like melting temperature[28]

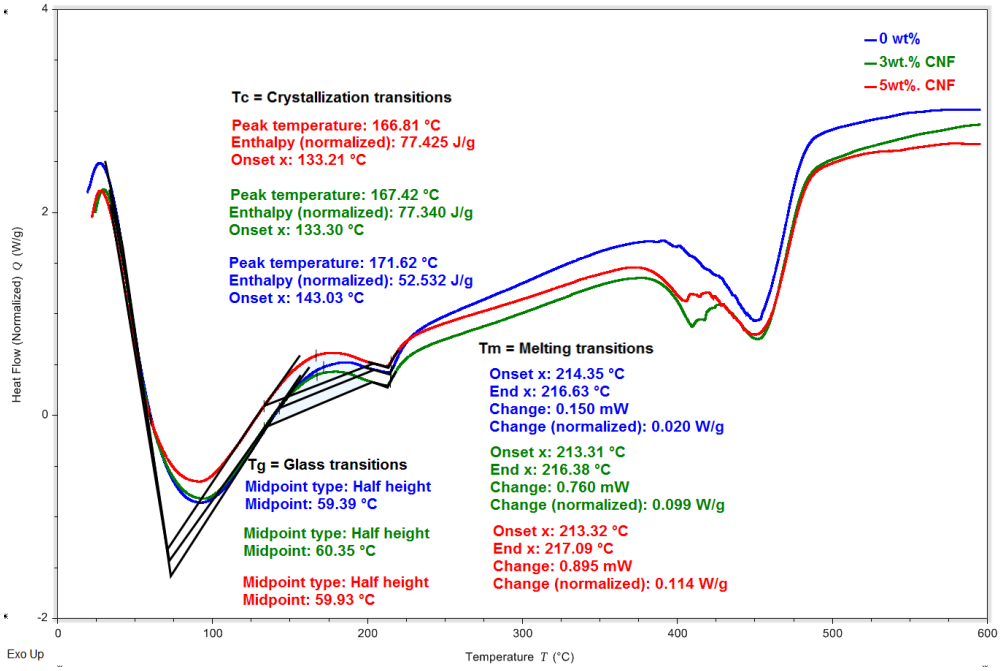

Figure 10: DSC Scan of PA6/CNF nanocomposites

The transition peak after the T_g illustrates the crystallization behavior of the investigated material system. The peak crystallization temperature was observed to be highest for the neat Nylon matrix, however, there was an early onset of crystallization at 3 and 5 wt.% respectively. This is expected and it is consistent with the Hoffman's nucleation theory which describes polymer crystallization in terms of kinetics and thermodynamics of surface nucleation[29]. The addition of CNF creates new surfaces in the nylon matrix thereby reducing the total surface energy of nuclei formation and consequently promoting heterogeneous nucleation which possesses a lower Gibbs free energy for crystallization. The heat of crystallization is the enthalpy associated with the crystallization process and could be used to determine the degree of crystallinity in the investigated material according to the following equation [26].

$$X_c\,(\%) = (\Delta Hm/(1-\varphi)\,\Delta H_o)\ X\ 100 \qquad (2)$$

Where ΔH_m is the enthalpy of crystallization melting shown in Figure 10, φ is the weight fraction of CNF, ΔH_o = 230 J/g is the consensual value reported in literature for the enthalpy of fusion of 100 % crystalline PA6 [30]. Using equation (1) the X_c (%) values have been computed as 22.8%, 34.6% and 35.4% of 0, 3 and 5 wt.% respectively of CNF loading. The observed increasing trend affirms the heterogeneous nucleation promoted by the carbon nanofibers. It is suspected that the higher degree of crystallinity experienced at 3 and 5wt% loading levels translated into the improvement of thermal stability and mechanical properties. However, the unusual deterioration of tensile properties of 5wt% could be due to possible weak interfacial strength vis-à-vis agglomeration effects.

The melting transitions in Figure 10 illustrates the onset of melting of the investigated material system. It could be observed that the onset of melting temperature slightly decreases with increasing CNF loadings. The presence of second phase CNF could promote increase in dislocation movements in the Nylon Matrix in form of interstices. These interstices could be perceived as weak impurities which lowers the melting temperature of the Nylon/CNF composites

4.6 Dynamic Mechanical Analysis

The DMA was used to evaluate the ability of the investigated material to return or store energy (storage modulus G'), dissipate energy (loss modulus G'') and the ratio of these effects (tan delta) signifies the transition from the glassy to rubbery state of the material. The storage modulus response observed in Figure 11 shows a trend like that of the tensile modulus plot. At 3wt.% loading of CNF, an improvement in the G' throughout the scanned temperature is an indication of the stiffening ability of CNF on the nylon matrix. The enhancements of storage modulus at 3wt% and 5wt% was more prominent at higher temperature, indicating the ability of CNF to enable the Nylon matrix to sustain its stiffness. This has been suggested to be due to interfacial interlocking between CNF and the polymer matrix which contributes to an additional reinforcement of restricted matrix molecular chain movement in the interface region of the nanocomposite[31]. The rapid decline in storage modulus in the transition region observed with increase in temperature could be attributed to a collective segmental motion of the chains in the polymer backbone, resulting into an energy dissipation phenomenon. The loss modulus illustrated in Figure 12 is an out-of-phase response which measures energy absorbed due to relaxation. The peak position of the loss modulus did not shift significantly at 3wt%, signifying that the inclusion of CNF has an insignificant effect on the dynamic relaxation behavior of the Nylon matrix [32]

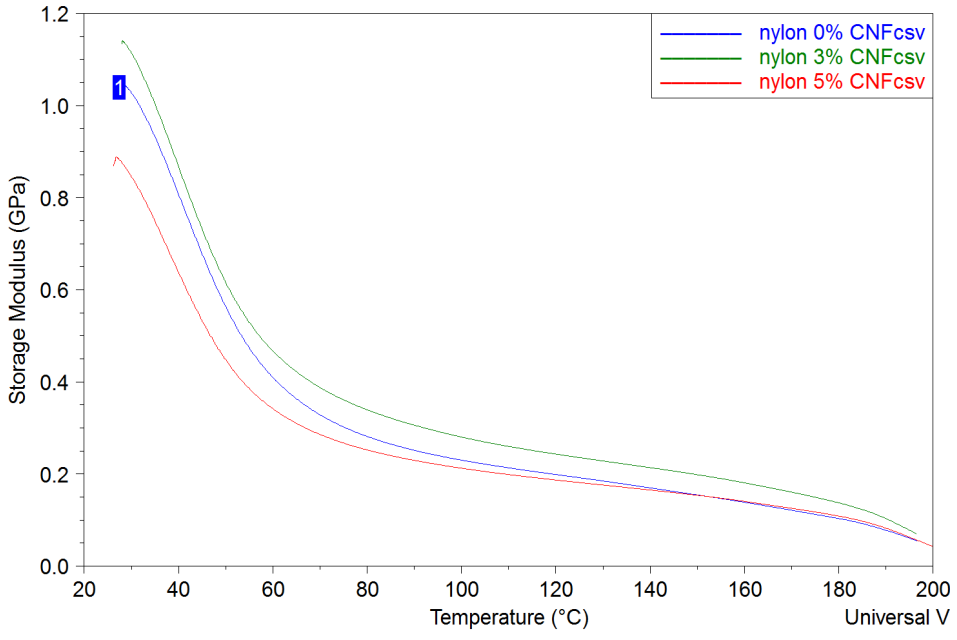

Figure 11: DMA thermograms of Storage modulus – Temperature Profile

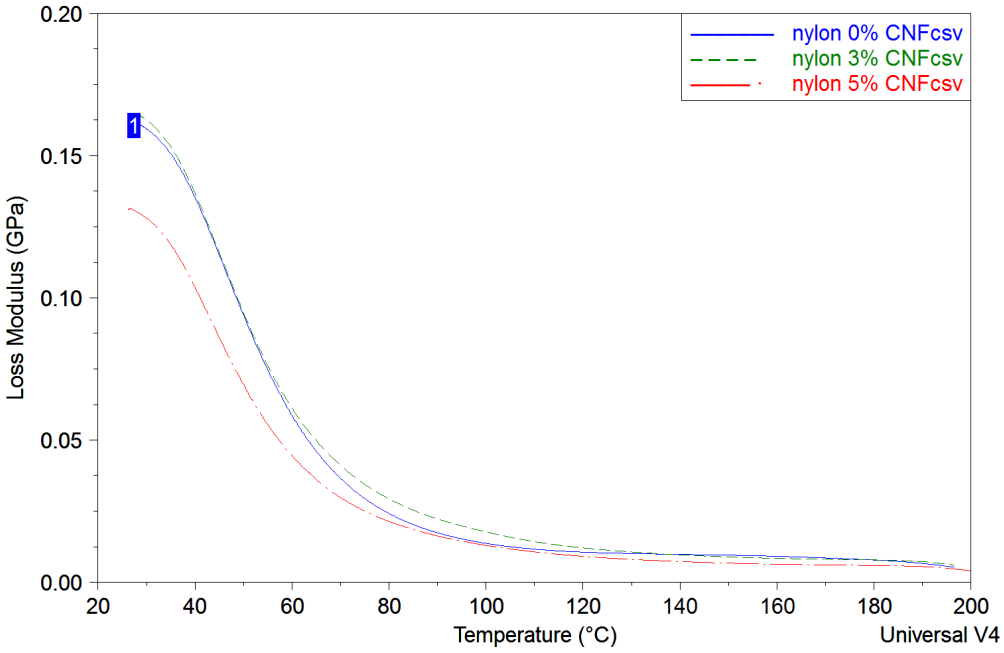

Figure 12: DMA thermograms of Loss modulus – Temperature Profile

The damping behavior of the investigated material were evaluated by the tangent of the phase angle (Tan Delta) which measures the ability of the material to absorbs energy. According to Figure 13, it could be observed that the area under the tan delta curve reduces with increasing CNF contents. This behavior is an indication of a homogeneous thermal energy distribution within the nylon/CNF nanocomposites that results from the high differential thermal conductivity between the CNF and Nylon matrix [26]

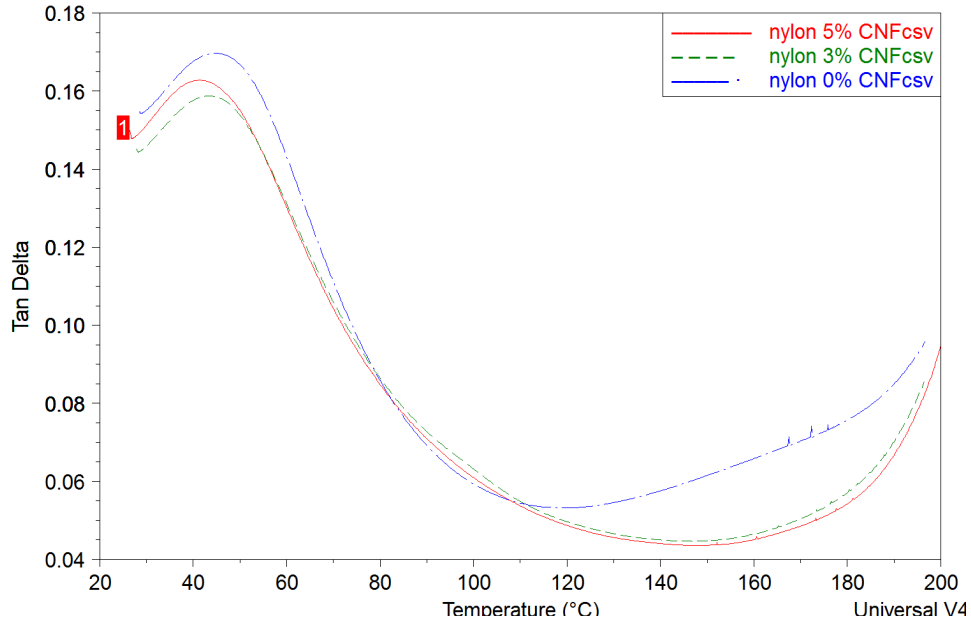

Figure 13: DMA thermograms of Tan Delta – Temperature Profile

5. CONCLUSION

PA6/CNF nanocomposite was successfully developed for 3D printing using co-rotating twin screw extruder for the compounding process. Fused deposition Modelling was used to manufacture test samples for mechanical, electrical and thermal properties investigation of the PA6/CNF nanocomposites. The following highlights are made from the results of this study.

i) There was an improvement of 11.4% tensile strength at 3wt% loading levels of CNF, however, 19% decrease of the tensile strength was observed when increasing the concentration of CNF to 5wt%. The agglomeration tendency of CNF is a well understood phenomenon and maximizing CNF potential at higher loading levels require optimizing the parameters of the manufacturing process.

ii) Significant improvement of 86.9% increment in the tensile modulus was observed at the 3wt% CNF loading. However, no significant effect was observed in the tensile modulus of 5wt%. This could be due to a porous interfacial strength for effective load transfer. There was an improvement of flexural properties with increasing CNF inclusion

iii) Carbon Nanofiber has proved to improve the electrical properties by lowering the volume resistivity of the insulating Nylon matrix. The volume resistivity observed at 3wt%. loading is quite significant and could be viable for electrostatic discharge application.

iv) The thermal properties of the nanocomposites were sustained with incorporation of CNF and no major deterioration was observed. No significant improvement in the thermal stability, weight percent loss, glass transition temperature of the nanocomposite. However, the crystallization transitions confirm higher degree of crystallinity with CNF inclusion.

v) It can be concluded from this study that the inclusion of CNF has shown high potential of developing a multifunctional PA6 nanocomposite for 3D printing, which could possess an excellent combination of mechanical, electrical and thermal properties. It is imperative to consider carrying out an extensive microstructural study via TEM to evaluate interfacial properties between the CNF and the Nylon matrix.

6. ACKNOWLEDGEMENTS

The authors would like to thank every members of Advanced Composites Lab, Texas State University for their accommodation while running the experiments of this research. We would also like to appreciate the help of Mr. Tom Taulman of 3D Taulman for providing us with adequate material.

7. REFERENCES

[1] L. W. McKeen, "7 - Polyamides (Nylons)," in *The Effect of UV Light and Weather on Plastics and Elastomers (Fourth Edition)*, L. W. McKeen, Ed.: William Andrew Publishing, 2019, pp. 185-222.

[2] (1998). *Aramids* [Online]. Available: http://www.pleo.com/dupont/nomex/.

[3] (2015). *Polyamides (Polylactams, Polyphthalamides and Polyaramids)* [Online]. Available: https://polymerdatabase.com/polymer%20classes/Polyamide%20type.html.

[4] X. Liu, R. Zhang, H. Zhu, and J. Wang, "Modeling method for battery distribution path optimization of EV charging and swapping service network," *Dianli Zidonghua Shebei/Electric Power Automation Equipment,* vol. 35, no. 6, pp. 10-16, 2015.

[5] W. Bauhofer and J. Z. Kovacs, "A review and analysis of electrical percolation in carbon nanotube polymer composites," *Composites Science and Technology,* vol. 69, no. 10, pp. 1486-1498, 2009/08/01/ 2009.

[6] L. Zonder, A. Ophir, S. Kenig, and S. McCarthy, "The effect of carbon nanotubes on the rheology and electrical resistivity of polyamide 12/high density polyethylene blends," *Polymer,* vol. 52, no. 22, pp. 5085-5091, 2011/10/13/ 2011.

[7] S. Gaikwad, J. Tate, N. Theodoropoulou, and J. Koo, "Electrical and mechanical properties of PA11 blended with nanographene platelets using industrial twin-screw extruder for selective laser sintering," *Journal of Composite Materials,* vol. 47, no. 23, pp. 2973-2986, 2013.

[8] P.-C. Ma, N. A. Siddiqui, G. Marom, and J.-K. Kim, "Dispersion and functionalization of carbon nanotubes for polymer-based nanocomposites: A review," *Composites Part A: Applied Science and Manufacturing,* vol. 41, no. 10, pp. 1345-1367, 2010/10/01/ 2010.

[9] A.-C. Brosse, S. Tencé-Girault, P. M. Piccione, and L. Leibler, "Effect of multi-walled carbon nanotubes on the lamellae morphology of polyamide-6," *Polymer,* vol. 49, no. 21, pp. 4680-4686, 2008/10/06/ 2008.

[10] R. Chávez-Medellín, L. A. S. d. A. Prado, and K. Schulte, "Polyamide-12/Functionalized Carbon Nanofiber Composites: Evaluation of Thermal and Mechanical Properties," *Macromolecular Materials and Engineering,* vol. 295, no. 4, pp. 397-405, 2010.

[11] W. Chanklin, "Electrical Properties Study of Carbon Fillers in Polymer Nanocomposites " Doctor of Philosophy Chemical Engineering, The University of New Brunswick, New Brunswick, Canada, 2016.

[12] A. Allaoui, S. V. Hoa, and M. D. Pugh, "The electronic transport properties and microstructure of carbon nanofiber/epoxy composites," *Composites Science and Technology,* vol. 68, no. 2, pp. 410-416, 2008/02/01/ 2008.

[13] F. K. Ko and Y. Wan, *Introduction to Nanofiber Materials*. Cambridge: Cambridge University Press, 2014.

[14] (2011). *Pyrograf III* [Online]. Available: http://pyrografproducts.com/Merchant5/merchant.mvc?Screen=cp_nanofiber.

[15] ASTM. (2014). *Standard Test Method for Tensile Properties of Plastics* [Online]. Available: https://www.astm.org/Standards/D638.htm.

[16] A. S. D790, " " Standard Test Methods for Flexural Properties of Unreinforced and Reinforced Plastics and Electrical Insulating Materials," ASTM International, West Conshohocken, PA," 2010.

[17] ASTM. (2014). *Standard Test Methods for DC Resistance or Conductance of Insulating Materials* [Online]. Available: https://www.astm.org/Standards/D257.htm.

[18] ASTM. (2017). *Standard Test Method for Thermal Stability by Thermogravimetry* [Online]. Available: https://www.astm.org/Standards/E2550.htm.
[19] ASTM. (2015). *Standard Test Method for Transition Temperatures and Enthalpies of Fusion and Crystallization of Polymers by Differential Scanning Calorimetry* [Online]. Available: https://www.astm.org/Standards/D3418.htm.
[20] ASTM, "Standard Practice for Plastics: Dynamic Mechanical Properties: Determination and Report of Procedures " 2012.
[21] G. Sui, W.-H. Zhong, M. A. Fuqua, and C. A. Ulven, "Crystalline Structure and Properties of Carbon Nanofiber Composites Prepared by Melt Extrusion," *Macromolecular Chemistry and Physics,* vol. 208, no. 17, pp. 1928-1936, 2007.
[22] N. Mahmood, M. Islam, A. Hameed, S. Saeed, and A. N. Khan, "Polyamide-6-based composites reinforced with pristine or functionalized multi-walled carbon nanotubes produced using melt extrusion technique," *Journal of Composite Materials,* vol. 48, no. 10, pp. 1197-1207, 2014.
[23] S. Y. Veena Choudhary and Anju Gupta , IntechOpen, . , "Polymer/Carbon Nanotube Nanocomposites, Carbon Nanotubes - Polymer Nanocomposites," 2011.
[24] L. Feng, N. Xie, and J. Zhong, "Carbon Nanofibers and Their Composites: A Review of Synthesizing, Properties and Applications," (in eng), *Materials (Basel),* vol. 7, no. 5, pp. 3919-3945, 2014.
[25] G. G. Tibbetts, I. C. Finegan, and C. Kwag, "Mechanical and electrical propertiesof vapor-grown carbon fiber thermoplastic composites," *Molecular Crystals and Liquid Crystals,* vol. 387, no. 1, pp. 129-133, 2002/01/01 2002.
[26] A. K. Barick and D. K. Tripathy, "Preparation and characterization of carbon nanofiber reinforced thermoplastic polyurethane nanocomposites," *Journal of Applied Polymer Science,* vol. 124, no. 1, pp. 765-780, 2012.
[27] T. H. Courtney, *Mechanical Behavior of Materials*, Second Edition ed. Waveland press, Inc, 2000.
[28] G. W. Ehrenstein and R. P. Theriault, *Polymeric materials : structure, properties, applications*. Munich; Cincinnati, OH: Hanser ; Hanser Gardner Publications, 2001.
[29] S. Z. D. Cheng and B. Lotz, "Enthalpic and entropic origins of nucleation barriers during polymer crystallization: the Hoffman–Lauritzen theory and beyond," *Polymer,* vol. 46, no. 20, pp. 8662-8681, 2005/09/23/ 2005.
[30] C. Millot, L.-A. Fillot, O. Lame, and P. Sotta, "Assessment of polyamide-6 crystallinity by DSC: Temperature dependence of the melting enthalpy," *Journal of Thermal Analysis and Calorimetry,* vol. 122, 04/09 2015.
[31] A. Eitan, F. T. Fisher, R. Andrews, L. C. Brinson, and L. S. Schadler, "Reinforcement mechanisms in MWCNT-filled polycarbonate," *Composites Science and Technology,* vol. 66, no. 9, pp. 1162-1173, 2006/07/01/ 2006.
[32] S. Yang, J. Taha-Tijerina, V. Serrato-Diaz, K. Hernandez, and K. Lozano, "Dynamic mechanical and thermal analysis of aligned vapor grown carbon nanofiber reinforced polyethylene," *Composites Part B: Engineering,* vol. 38, no. 2, pp. 228-235, 2007/03/01/ 2007.